

## Microscopic coupled-channel description of pion inelastic scattering from rotational nuclei

Johann Bartel,\* Mikkel B. Johnson, Mano Singham,<sup>†</sup> and Wilhelm Stocker<sup>‡</sup>

*Los Alamos National Laboratory, Los Alamos, New Mexico 87545*

(Received 4 October 1993)

We establish the applicability of a microscopic coupled-channel theory to pion inelastic scattering from rotational nuclei for the purpose of studying details of neutron and proton densities. The theory is completely specified as a result of our taking the second-order pion-nucleus optical potential from previous phenomenological studies of elastic and charge-exchange data on spherical nuclei and of our using nuclear wave functions obtained from a Hartree-Fock + BCS calculation with the Skyrme SKM\* interaction. Making multipole expansions leads to a set of coupled equations, which is solved for the scattering cross sections in a standard manner. Numerical studies are presented for the specific nucleus  $^{152}\text{Sm}$ . The theory is shown to be stable with respect to truncation of the expansions: we find rapid convergence of the cross sections for elastic scattering and inelastic scattering to the first  $2^+$  and  $4^+$  states as transition densities of successively higher multipolarity are added, and as the number of coupled rotational nuclear levels is increased. Medium modifications are included and have a small but significant effect on the cross section: for scattering to the  $2^+$  state, their effect is about 10% for both  $\pi^-$  and  $\pi^+$ . We also quantify the extent of sensitivity of pion scattering cross sections to variations in the size and shape of the neutron and proton distribution using parametrized Woods-Saxon forms for the density.

PACS number(s): 25.80.Ek, 24.10.Eq

### I. INTRODUCTION

The use of the pion as a selective probe of the nuclear neutron density is suggested by the fact that for pions of energy near 180 MeV (i.e., in the vicinity of the strong  $\Delta_{33}$  resonance that occurs in the  $p$ -wave pion-nucleon scattering amplitude), the negative pions scatter more strongly from neutrons and the positive pions more strongly from protons. Such studies have been made possible as a result of the development of the intense beams of pions available at the meson factories. Sensitivity of resonance-energy pions to the neutron distribution in the nuclear surface was substantiated by early studies of total cross sections [1] and of cross sections for elastic scattering [2]. Experimental studies of pion inelastic [3] and charge exchange [4] scattering on the deformed nuclei  $^{152}\text{Sm}$  and  $^{165}\text{Ho}$ , respectively, were motivated by interest in the shape of neutron densities.

A theoretical framework for describing pion scattering from deformed nuclei was proposed earlier [5] in connection with measurements [4] of charge exchange on aligned  $^{165}\text{Ho}$ . It is the purpose of the present paper to apply the same theory to inelastic scattering from deformed nuclei

and to document its applicability for the purpose of distinguishing details of densities from such measurements in the particular case of  $^{152}\text{Sm}$  [3].

In extending the theory from spherical to deformed nuclei, a new level of complexity arises having to do with the pion's ability to couple the ground and excited states through the off-diagonal terms of the optical potential. The manageability of the theory for exploring densities with a given probe is very much dependent on knowing its stability when this coupling is turned on. The concern is well appreciated, but the importance of the coupling will differ from probe to probe. Some of the intricacies have been carefully studied for protons [6] and  $K^+$  mesons [7]. The case of the pion at resonance is expected to be different because of its substantially stronger coupling to the nucleon. We are able to provide an absolute calibration in this case by virtue of the facts that (1) the optical potential we use is completely specified by earlier studies of  $\pi^\pm$  scattering from spherical nuclei, and (2) the nuclear structure we use has been obtained from a Hartree-Fock BCS theory using the SKM\* interaction [8], which has been carefully crafted especially with respect to surface properties. Otherwise, the pion is favorably positioned in comparison to the proton and  $K^+$  as a probe of nuclei, with extensive data sets available for elastic  $\pi^\pm$  and charge exchange on both nucleons and nuclei.

We stress that the use of realistic wave functions is crucial to avoid a misleading assessment of the behavior of the theory for resonance-energy pions, for which the surface region of the nucleus is particularly emphasized. As neutron densities are not measured, one must rely on theory to provide the wave functions. For the particular case of SKM\*, the interaction has been designed to re-

\*Present address: Université Louis Pasteur and CRN de Strasbourg/PNth, B.P. 20, F-67037 Strasbourg, France.

<sup>†</sup>Present address: Department of Physics, Case Western University, Cleveland, OH 44106.

<sup>‡</sup>Present address: Sektion Physik, Universität München, D-8046 Garching, Germany.

produce ground-state energies, root-mean-square charge radii, isoscalar monopole and isovector electric dipole ( $E1$ ) giant resonance data as well as actinide fission barriers. Furthermore, Hartree-Fock theories have done an impressive job of explaining electron scattering data throughout the periodic table, so we might reasonably expect that the theory we use would give a reasonable description of properties of neutrons and protons in the surface of  $^{152}\text{Sm}$ . The technology for solving HF equations for nuclei has become standard, allowing *ab initio* calculations of deformed nuclei for given effective interactions (see Ref. [9] for a review).

Establishing the applicability of the theory [5] to inelastic scattering for the purpose of distinguishing details of neutron and proton densities entails a careful study of several issues. The issue of convergence arises because various multipole expansions are made to obtain the coupled equations. We will study in Sec. IV the convergence of the theory with respect to the number of multipoles included in the decomposition of the HF density as well as with respect to the number of coupled intermediate rotational states. In the model of Ref. [3] excited rotational levels were important even for the  $2^+$ , and our work was motivated in part by this observation. In addition, we want to understand the impact of the medium modifications, which occur in the optical potential that we use [5] but were not available for the earlier study [3]; we present our discussion of the medium modifications in Sec. V. Having established the importance of these effects, we finally study in Sec. VI the sensitivity of the cross section to variation of the density in our theory. Application of the theory to the experimental data on pion scattering from  $^{152}\text{Sm}$  is presented in a separate publication [10].

## II. THEORY

The theory on which we base the current investigation was described in Ref. [5], and we refer the reader to this paper for the details. It utilizes a microscopic optical model of the form originally suggested by Ericson and Ericson [11], and it has been applied to pion elastic and charge-exchange scattering both at low energy [12] and in the region of the 3-3 resonance [13] for spherical nuclei. The theory is based on an optical model theory for closed-shell nuclei and assumes that the nucleon motion inside the nucleus is well described in the mean-field approach.

The use of microscopic pion scattering theory to study nucleon densities is complicated by the fact that the pions may interact with collections of two-or-more nucleons in nuclei. This gives rise to corrections to the simple picture of multiple scattering as a succession of pion interactions with individual neutrons and protons. These corrections appear in the optical potential as terms nonlinear in the neutron and proton densities. The strengths of these corrections are difficult to calculate from first principles, but they can be quite important because they modify the relative sensitivity of pions to neutrons and protons. The framework that we apply here [5] addresses this issue through phenomenological isoscalar and isovector terms

quadratic in the nuclear density. In the resonance region, the quadratic isovector terms must be quite large to agree with the single-charge-exchange data [13]. Such corrections were not available for the earlier studies [3], and we have been particularly interested in quantifying their effect for inelastic scattering.

For the current application, only the isoscalar  $U_0$  and isovector optical potential  $U_1$  are required,

$$U = U_0 + U_1 \frac{\boldsymbol{\phi} \cdot \mathbf{T}}{2T}. \quad (2.1)$$

Here,  $\boldsymbol{\phi}$  is the isospin operator for the pion and  $\mathbf{T}$  is the isospin operator of the nuclear ground state. A density expansion [14] has been used to express the optical potential as a series in powers of the total density  $\rho(\mathbf{r}) = \rho_n(\mathbf{r}) + \rho_p(\mathbf{r})$  (here  $\rho_n(\mathbf{r})$  and  $\rho_p(\mathbf{r})$  are the neutron and proton densities, respectively) and  $\Delta\rho(\mathbf{r}) = \rho_n(\mathbf{r}) - \rho_p(\mathbf{r})$ . For charge-exchange scattering,  $\Delta\rho(\mathbf{r})$  is defined as the excess neutron density, defined below [see Eq. (2.7)]. In our HF + BCS model the neutron and proton density is

$$\rho_q(\mathbf{r}) = \sum_i |\Psi_{iq}(\mathbf{r})|^2 v_{iq}^2, \quad q = n, p, \quad (2.2)$$

where the sum runs over all the orbitals  $i$  which are occupied with an occupation probability  $v_q^2$ . These densities have a deformed shape, so the optical potential employing these densities is also deformed. In order to solve the corresponding Klein-Gordon scattering equation, we expand both the densities and the scattering wave function in multipoles. Thus, each density  $\rho$  (neutron, proton, or excess neutron density) can be expressed as

$$\begin{aligned} \rho(\mathbf{r}) &= \rho^{(0)} + \delta\rho(\mathbf{r}) \\ &= \rho^{(0)} + \sum_{\lambda>0} \rho^{(\lambda)}(r) Y_{\lambda 0} \sqrt{4\pi(2\lambda+1)}, \end{aligned} \quad (2.3a)$$

where

$$\rho^{(\lambda)}(r) = \frac{1}{4\pi} \int_0^{2\pi} d\phi \int_0^\pi d\theta \sin\theta \rho(r, \theta) P_\lambda(\cos\theta). \quad (2.3b)$$

Here  $\rho^{(0)}(r)$  is the monopole component of the density, and  $\delta\rho(\mathbf{r})$  [whose explicit form follows directly from Eqs. (2.3a) and (2.3b)] is one piece of the transition density appearing in Eq. (2.5) below.

The rotational model, which is valid for strongly deformed nuclei such as  $^{152}\text{Sm}$ , allows us to identify the multipole components of the nuclear density with transition densities to rotational levels of the target nucleus. Corresponding to the substitution in Eq. (2.3a) the optical potential undergoes a change,

$$U \rightarrow U + \delta U. \quad (2.4)$$

The optical potential  $U$  now describes scattering from the monopole piece of the density and  $\delta U$  the piece of the pion-nucleus interaction that induces transitions among the rotational levels. The effect of the  $\delta U$  enters into both the elastic and inelastic scattering. When it occurs in the diagonal (elastic) channels, it is referred to as reorientation coupling.

Since  $U$  is a functional of  $\rho$  and  $\Delta\rho$ , we can find  $\delta U$  in Eq. (2.4) by taking derivatives of  $U$  with respect to density. If the transition optical potential for inelastic scattering is taken to be linear in the small quantities  $\delta\rho$ ,  $\Delta\rho$ , and  $\delta(\Delta\rho)$  [15,16], then

$$\delta U = \delta\rho \frac{\partial}{\partial\rho} U_0 + \delta(\Delta\rho) \frac{\partial}{\partial(\Delta\rho)} U_1 \frac{\boldsymbol{\phi} \cdot \mathbf{T}}{2T}, \quad (2.5)$$

where we have used the fact that  $U_1$  has all the dependence on  $\Delta\rho$ .

The transition potential for single charge exchange, which we do not calculate here, is given by

$$\delta U = \delta(\Delta\rho) \frac{\partial}{\partial(\Delta\rho)} U_1 \frac{\boldsymbol{\phi} \cdot \mathbf{T}}{2T}, \quad (2.6)$$

where in this case  $\Delta\rho$  is the transition density to the isobaric analog state. This is given in terms of the Hartree-Fock wave functions and occupation probabilities [5] as

$$\Delta\rho(\mathbf{r}) = \sum_i (v_{in}^2 - v_{ip}^2) \Psi_{ip}^*(\mathbf{r}) \Psi_{in}(\mathbf{r}). \quad (2.7)$$

We see from Eqs. (2.5) and (2.6) that the optical potential for inelastic scattering of  $\pi^+$  and  $\pi^-$  is sensitive to a linear combination of both the neutron and the proton density. For scattering near the 3-3 resonance, if we ignore the medium modifications, one finds that  $U_0$  is proportional to  $\rho$  and  $U_1$  to  $\Delta\rho$  with coefficients that are about the same size. Since  $\boldsymbol{\phi} \cdot \mathbf{T}/2T$  is  $-1/2$  for  $\pi^+$  and  $+1/2$  for  $\pi^-$ , we then see that for  $\pi^+$  the protons dominate by about a factor of 3 and for  $\pi^-$  the neutrons dominate by the same amount. Moreover, we also see from Eqs. (2.3) and (2.5) that it is not the full density that enters  $\delta U$ , but rather the multipole densities, so that the optical potential for inelastic scattering is proportional to the respective deformation parameter  $\beta_\lambda$  of that density. Thus, to the extent that coupled-channel effects are small, the inelastic cross section for  $\pi^+$  is selectively sensitive to multipole density of protons and  $\pi^-$  to the multipole density of neutrons. In contrast, the charge-exchange scattering is driven by the multipole density of the excess neutrons [see Eqs. (2.6) and (2.7)], which according to the above discussion gives another closely related piece of information about the nuclear structure. Later we shall assess numerically the extent to which these conclusions hold when medium modifications and channel-coupling effects are considered.

### III. DENSITIES

For the scattering calculations that we present in Sec. IV and V below, we use the numerical HF densities. However, for our study in Sec. VI of the sensitivity of cross sections to changes in the density, we will not be able to use the HF densities because we do not have freedom to vary the size or shape of the nucleus in the SKM\* HF theory. Instead, we will be making variations using a parametrized representation of the density in terms of

Fermi functions (Woods-Saxon form). Next we compare the multipole decomposition of the HF densities and the corresponding Woods-Saxon parametrization obtained as described below. This will form the basis of the study in Sec. VI.

In Figs. 1–3 we illustrate the multipole densities for the case of the neutrons. The solid lines are the SKM\* HF densities calculated from Eq. (2.3c) for  $^{152}\text{Sm}$ . The long dashed curves are the multipole decomposition of the equivalent Woods-Saxon densities,

$$\rho(\mathbf{r}) = \frac{\rho_0}{1 + e^{(r-R)/a}}, \quad (3.1a)$$

with

$$R = R_0 \left[ 1 + \sum_{\lambda>0} \beta_\lambda Y_{\lambda 0}(\theta, \phi) \right]. \quad (3.1b)$$

Here  $a$  is the surface thickness, assumed to be independent of  $\theta$ . The deformation parameters  $\beta_\lambda$  were determined through the condition that the distribution in Eq. (3.1) has multipole moments  $Q_\lambda$  identical to those obtained self-consistently in the HF approach. The corresponding central density  $\rho_0$ , half-density radius  $R_0$ , and  $a$  were then adjusted to match the Woods-Saxon distribution to the (three-dimensional) HF density. Particle-number conservation, which amounts to a constraint between  $\rho_0$ ,  $R_0$ , and  $a$ , was imposed in making the fit. The resulting density parameters and multipole moments are shown in Table I [17]. The Woods-Saxon multipole decomposition given by the long-dashed curve is evaluated numerically with Eq. (2.3b). Finally, the dotted line is the lowest-order Taylor expansion approximation of the multipole decomposition of the Woods-Saxon density,

$$\rho^{(0)}(r) = \frac{\rho_0}{1 + e^{(r-R)/a}} \quad (3.2a)$$

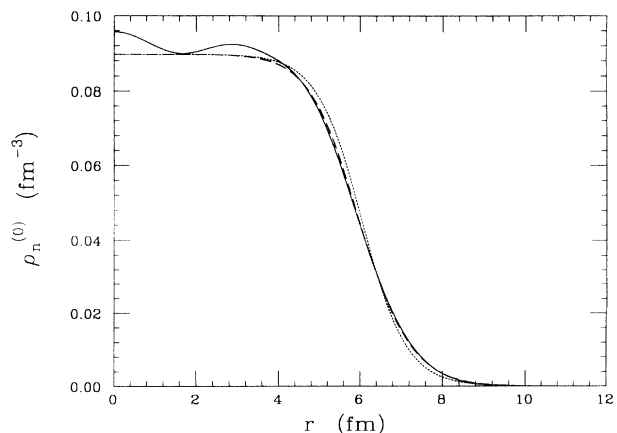


FIG. 1. Monopole part  $\rho_n^{(0)}$  of the SKM\* HF neutron density for  $^{152}\text{Sm}$  (solid line) in comparison with the monopole density obtained with Eq. (2.3c) from the Woods-Saxon density fitted to the HF density (dashed line) and the approximation of Eq. (3.2) (dotted line).

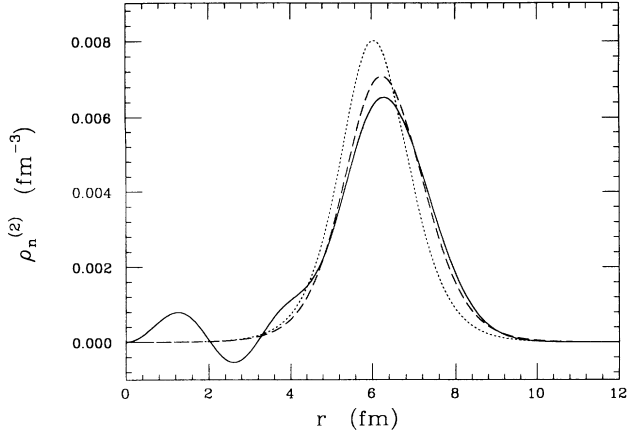


FIG. 2. Same as Fig. 1 for the quadrupole density  $\rho_n^{(2)}$ .

$$\rho^{(\lambda)} = -\frac{R_0 \beta_\lambda}{\sqrt{4\pi(2\lambda+1)}} \frac{d}{dr} \rho^{(0)}(r). \quad (3.2b)$$

From these figures, we see that the lowest-order Taylor expansion is not a good approximation to the shape of the full numerical multipole decomposition [Eq. (2.3b)] at least for highly deformed nuclei [18]; for this reason, we will not make use of the Taylor expansion in this work.

According to the figures, the exact multipole decomposition of the Woods-Saxon densities of Eq. (3.1a) appears to be a good representation of the corresponding Hartree-Fock densities, particularly in the nuclear surface. For the purpose of pion scattering in the resonance region (corresponding to the experiment in Ref. [3]), the two densities will give very similar angular distributions. It is clear, for example, that the pattern of diffraction oscillations will be nearly identical because for these the important densities are those beyond the 10% density point [2], which is essentially the same for the HF and Woods-Saxon distributions.

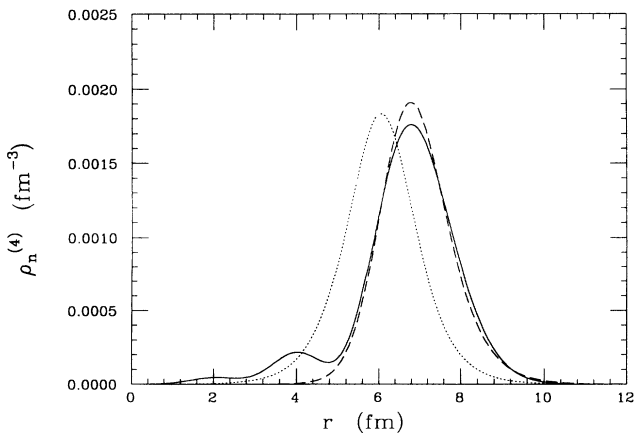


FIG. 3. Same as Fig. 1 for the hexadecapole density  $\rho_n^{(4)}$ .

TABLE I. Parameters of the equivalent Woods-Saxon densities.

	$\beta_2$ $Q_2$ (fm <sup>2</sup> )	$\beta_4$ $Q_4$ (fm <sup>4</sup> )	$\beta_6$ $Q_6$ (fm <sup>6</sup> )	$R_0$ (fm)	$a$ (fm)
Neutrons	0.2578 810.04	0.0790 14406	0.0030 242170	6.05	0.55
Protons	0.2897 603.40	0.0747 9699	0.0032 162420	5.95	0.5

#### IV. CONVERGENCE OF MULTIPLE SCATTERING THEORY

The use of HF densities gives us a complete model of the nuclear size and shape and thus provides the opportunity to study the convergence of the multiple scattering expansion in the rotational model. There are two aspects to the study of the convergence. One of these concerns the convergence with respect to the number of rotational nuclear states coupled together. The other concerns the convergence as the number of multipoles included in Eq. (2.3) is increased. The results we give below are for  $\pi^-$  scattering, but similar calculations have been performed for  $\pi^+$ , and we find effects following the same trend with regard to sign and magnitude.

##### A. Convergence with respect to number of nuclear states

We will first look at the convergence for a given rotational final state  $F$  characterized by total angular momentum  $J$  and parity  $P$  (denoted by  $J_F^P$ ) as a function of the selection of coupled rotational states  $C$  (designated by  $J_C^P$ ). For this purpose we have retained the first four of the multipole densities ( $\lambda = 0, 2, 4, 6$ ) for the off-diagonal transitions. As we will see in Sec. IV B, the convergence with increasing  $\lambda$  is rather rapid for a nucleus as strongly deformed as  $^{152}\text{Sm}$ . We have not included the reorientation couplings for this study (for a discussion of the size of the reorientation coupling see Sec. IV B 1).

We will discuss results for the cross sections for the  $J_F^P = 0^+, 2^+, \text{ and } 4^+$  final states. To study the convergence we coupled successively (as appropriate) the  $J_C^P = 2^+, 4^+, \text{ and } 6^+$  rotational states. We had some difficulty in carrying out the complete  $J_C^P = 6^+$  calculation, because the storage and running time requirements became quite demanding. We have found that there is very little change in either the elastic scattering or the inelastic scattering to the  $2^+$  final state as these intermediate states are coupled. We do not show figures for these cases because they all look the same on graph paper. The  $4^+$  final state is interesting, and the results are shown in Fig. 4. Note that there is a strong destructive interference between the direct excitation of the  $4^+$  state (dotted curve) and the indirect coupling through the  $2^+$  state, the dashed curve giving the sum of these two amplitudes. Similar types of interference have been noted

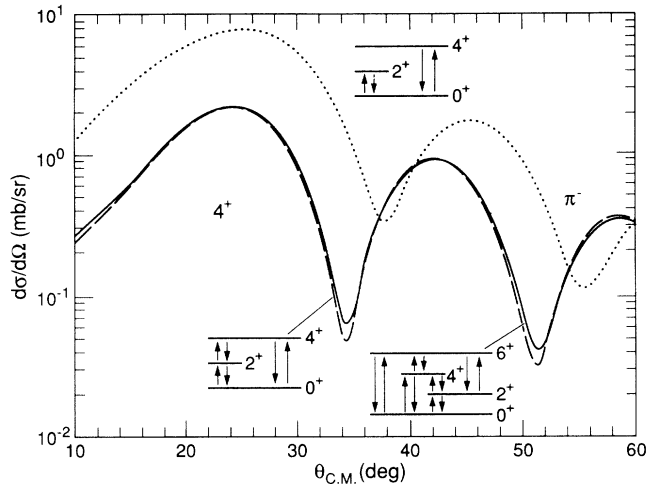


FIG. 4. Study of the rate of convergence of the  $\pi^- 4^+$  cross section with respect to the number of states coupled (see insets).

as possible explanations of  $\alpha$ -particle scattering angular distributions [19]. Addition to the  $6^+$  intermediate state (solid curve) makes less than 10% additional change.

It would be interesting to measure the scattering to the  $4^+$  state because of the destructive interference between the direct scattering to this state through the  $\lambda = 4$  density multipole and the two-step scattering through  $2^+$  state as seen in Fig. 4. Because of the resulting cancellations, the experimental results are quite sensitive to details and will provide an interesting test to the underlying nuclear structure and reaction theory. This sensitivity has been exploited for the case of  $\alpha$ -particle scattering on the Ti isotopes to test shell-model selection rules [20].

## B. Convergence with respect to the number of multipoles

There are two aspects of the convergence with respect to the number of multipoles, and we will look at these separately. One is the convergence with respect to the number of multipoles in the diagonal (reorientation) coupling, and the other with respect to the number of off-diagonal couplings.

### 1. Diagonal (Reorientation) Coupling

We have found that elastic scattering is rather insensitive to whether or not reorientation coupling is included. Because its effect on elastic scattering is so small, we do not present a figure showing the results. Reorientation coupling is somewhat more important for scattering to the  $2^+$  state, and the result of this calculation is shown in Fig. 5(a). The results for the reorientation coupling corresponding to the  $\lambda = 2$  multipole and  $\lambda = 2 + 4$  multipoles are shown separately. The largest effect is for  $\lambda = 2$ , which gives a 20% decrease of the peak cross sec-

tion. Adding the  $\lambda = 4$  multipole leads to an additional 10% decrease.

In Fig. 5(b) we show the effect of the reorientation coupling on the scattering to the  $4^+$  final state. We have already seen that a strong destructive interference occurs between direct scattering to the  $4^+$  and scattering to the  $4^+$  through the intermediate  $2^+$  state. Thus, we present separately results showing the influence of reorientation coupling on the  $4^+$  and on the  $2^+$  states involved in this transition. The dotted curve in Fig. 5(b) is the case with no reorientation coupling, and as such it is the same as the solid curve in Fig. 4. Including reorientation coupling only in the intermediate  $2^+$  state gives the short-dashed

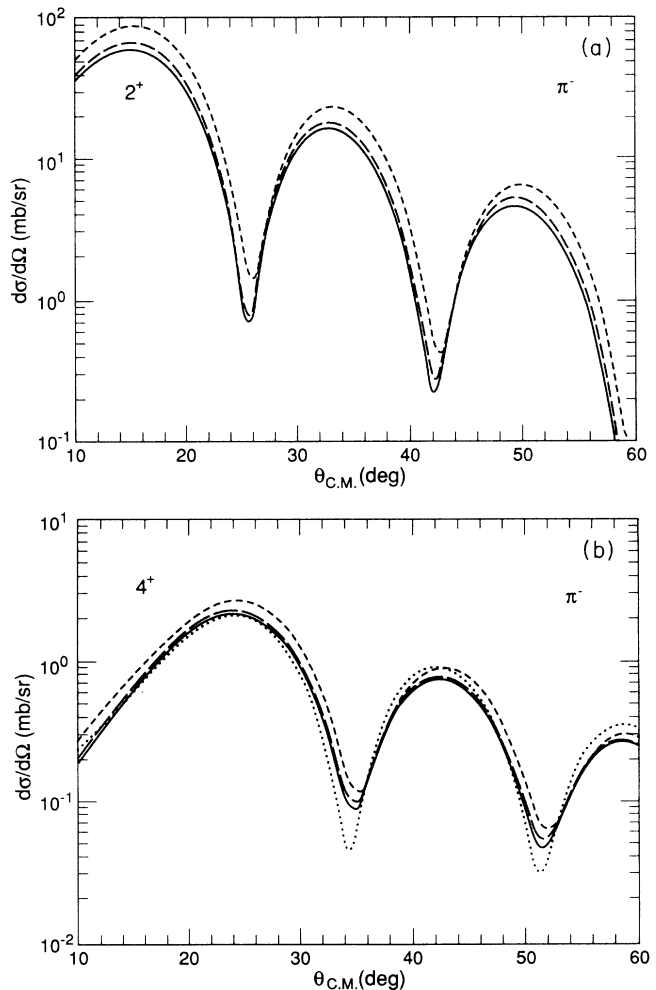


FIG. 5. Study of the importance of reorientation coupling in the  $\pi^-$  (a)  $2^+$  cross section and the (b)  $4^+$  cross section. In (a) the short-dashed curve is obtained without reorientation coupling, the dashed curve has  $\lambda = 2$  orientation coupling included and the continuous curve has in addition  $\lambda = 4$  included. In (b) the dotted curve is obtained without reorientation coupling. The short-dashed curve has reorientation coupling in the  $2^+$  state but not the  $4^+$  state. The remaining curves have reorientation coupling in the  $2^+$  state and various multipoles  $\lambda$  in the  $4^+$  state: the long-dashed curve has  $\lambda = 2$  in the  $4^+$  state, and the continuous curve  $\lambda = 2 + 4$ ; including  $\lambda = 6$  in the  $4^+$  leads to no further change.

curve. This gives rise to a small increase in the cross section to the  $4^+$  final state.

The remaining curves of Fig. 5(b) show the effect of including the reorientation coupling in the  $4^+$  state successively through the  $\lambda = 2$ ,  $\lambda = 2+4$  and to  $\lambda = 2+4+6$  multipoles as indicated in the figure caption. Here, we see that the sequence of calculations converges rather rapidly. The final result, including full reorientation coupling in the  $2^+$  and  $4^+$  states involved in the transition, resembles (except near the cross section minima) the short-dotted calculation, which included no reorientation coupling.

## 2. Off-diagonal coupling

Given the results described in Sec. IV A above, namely that the coupling of excited rotational states  $J_C^P$  does not have an appreciable effect on the ground state and first excited  $2^+$  state, it is clear that the differential cross section cannot be sensitive to the off-diagonal couplings, which are responsible for the transitions among these excited rotational states.

We have seen in Fig. 4 that the  $4^+$  state is sensitive to the coupling scheme, so the off-diagonal couplings have their first chance to be important for this state. The results are shown in Fig. 6. We see here that the  $\lambda' = 4$  multipole is relatively important for the  $4^+$  state, but that the  $\lambda' = 6$  multipole is not.

## C. Discussion

We have found that the importance of the diagonal and off-diagonal couplings decrease with increasing multipolarity. Thus, we find as an approximate rule that the

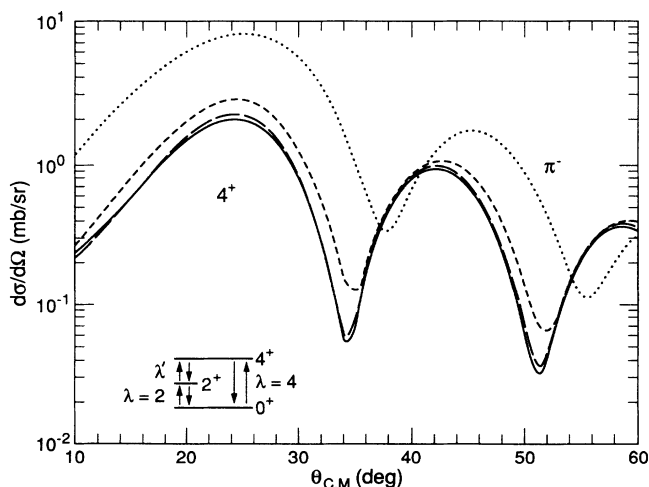


FIG. 6. Off-diagonal coupling. Study of the convergence of the  $4^+$  cross section with respect to the multipoles  $\lambda'$  included in the  $2^+ \rightarrow 4^+$  coupling scheme (see inset). The dotted curve has no coupling between the  $2^+$  and  $4^+$  states. The short-dashed curve has  $\lambda' = 2$ , the long-dashed curve  $\lambda' = 2 + 4$ , and the solid curve  $\lambda' = 2 + 4 + 6$ .

convergence is about as fast as can be expected: states up to  $J_C^P = J_F^P$  are the most important diagonal and off-diagonal term in the interaction. We refer to this as the minimal coupling scheme. We tried to check the rule for the case of the  $6^+$  final state, but because of time and storage limitations we were unable to reach a firm conclusion for this case.

The coupling to excited rotational states does not influence very strongly the calculation of the cross section for pion scattering from the ground state or  $2^+$ , and in this sense the coupled-channel approach is equivalent to the DWIA theory for the  $2^+$  state. However, because of the importance of reorientation coupling for the  $2^+$ , a standard DWIA-type calculation would not provide quantitatively accurate values for the cross sections. In general the coupling to excited states is necessary, as illustrated by the case of pion scattering to the  $4^+$  state, where this aspect was shown to be very important.

Although part of our original motivation arose from the observation in Ref. [3] that coupling of excited rotational levels is important for the calculation of the cross section to the  $2^+$  final state, we have concluded that in our theory convergence is sufficiently rapid so that this coupling is in fact unimportant [21]. Nevertheless, in line with the discussion of the previous paragraph, we still need to retain the coupled-channels capability in order to take account of the moderately important reorientation coupling.

## V. EFFECT OF MEDIUM-MODIFICATIONS IN THE OPTICAL POTENTIAL

The sources of medium-modifications in the optical potential are the terms that are nonlinear in density, described in Sec. II. The coefficient of the isoscalar  $\rho^2$  term is relatively small, but the coefficient of the isovector  $\rho\Delta\rho$  term is quite large. The small size of the isoscalar piece has been explained in Ref. [22] as the result of an approximate cancellation between the Pauli effect, which effectively narrows the resonance, and collision-broadening terms. Corrections arising from kinetic and potential energies of the nucleon and delta also occur. Some cancellations among these take place [22]; in the present theory, the net effect is included as a shift in the energy of the pion-nucleon scattering amplitude rather than as a density-dependent term.

In previous studies of pion inelastic scattering one has tended to use the lowest-order optical potential to determine the inelastic scattering. Ignoring the medium modifications may lead to spurious conclusions regarding both the absolute and relative sizes of the neutron and proton densities, depending of course on the size of the medium effects. For example, as much as a 10% change in the relative size of the cross section for scattering of  $\pi^+$  and  $\pi^-$  to the  $2^+$  state can be significant in an attempt to ascertain whether there is a difference between the neutron and proton deformation, since differences between the deformations are of this same size [10]. The relative cross section is of course influenced by the isovector rather than the isoscalar terms. Our cur-

rent theory provides us with an opportunity to quantify the importance of these medium modifications in the determination of the neutron distributions from inelastic excitation of rotational levels in  $^{152}\text{Sm}$ .

Figures 7(a) and 7(c) show the net influence of both the isoscalar and isovector medium modifications on elastic scattering, and Figs. 7(b) and 7(d) show their effect on inelastic scattering to the  $2^+$  state. We see that the medium modifications have a significant effect, increasing the scattering to the  $2^+$  state by about 10% (except in the minima, where the effect is quite a bit larger). Because the medium modifications change  $\pi^+$  and  $\pi^-$  in much the same way, one sees that the dominant source of the differences between the solid (with medium modifications) and dashed (without medium modifications) curves can be traced to the nonlinear terms contributing to the isoscalar piece of the optical potential. For this reason, they will not have much impact on the conclusion about the relative size of neutron and proton deformations. We find medium modifications have a substantially

larger effect (about a factor of 2) on the scattering to the  $4^+$  state. The isoscalar medium modifications again dominate.

For single charge exchange, in contrast to Fig. 7, the effect of the isovector medium modifications is to increase the overall cross sections by roughly a factor of two [5,13]. Isovector medium modifications thus have, perhaps, a surprisingly small effect on inelastic scattering. One reason for the difference is that single-charge-exchange scattering occurs entirely through the isovector pieces of the optical potential. On the other hand, in Fig. 7 the optical potential is dominated by the  $N = Z$  core, where the isoscalar optical potential dominates, with the isovector terms not contributing at all.

For the case of scattering to the  $2^+$  state, an additional reason can be found for the medium modifications being small, namely that the transition density is peaked rather far out in the nuclear surface, near the half-density point. One can see how far out in the surface the  $2^+$  transition density extends by comparing the monopole and  $2^+$

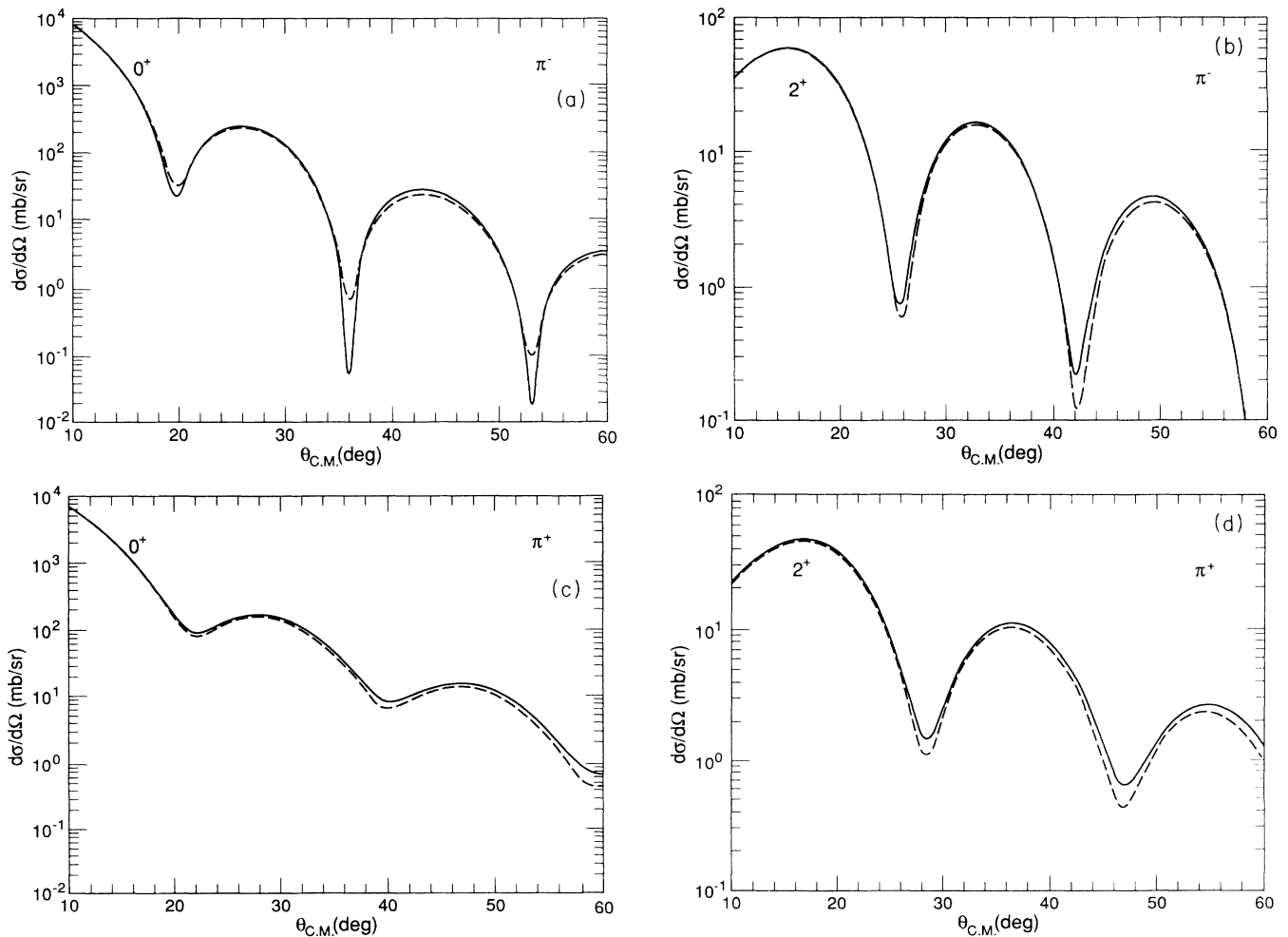


FIG. 7. Illustrating the importance of medium modifications in the optical potential for (a) [and (c)] the elastic and (b) [and (d)]  $2^+$  the cross section for  $\pi^-$  (and  $\pi^+$ ). No coupled excited states are taken into account, but reorientation coupling is fully included. The dashed curves are for the first-order optical potential, and the full curves take account of the isoscalar and isovector (density-dependent) medium modifications.

transition densities given in Figs. 1 and 2, respectively. We see that a substantial contribution comes from radii greater than the 10% density, where the medium modifications are small due to the extra factor of density compared to the lowest-order terms of the optical potential.

Suppression of the medium modifications by this mechanism is even more pronounced for the  $4^+$  multipole. Recall that the scattering amplitude for the  $4^+$  final state results from a strong destructive interference between direct excitation and a two-step excitation through the  $2^+$  (Fig. 4). Presumably the influence of medium modifications on the  $4^+$  transition is magnified by the destructive interference between these two amplitudes and is responsible for the large effect that we have found here.

## VI. SENSITIVITY TO VARIATIONS OF DENSITIES

As we explained in Sec. III, we do not have a means to vary the radius, diffuseness, and deformation of the nucleus independently and will therefore use the collective parameterization of the Woods-Saxon densities given in Eq. (3.1) for the studies of the sensitivity to variation of the densities. The parameters of the Woods-Saxon density are found in Table I. For the results presented in this section we include the medium modifications and work within the “minimal” coupling scheme defined at the end of Sec. IV.

It is known from previous studies of diffractive elastic scattering that the location of the minima and the rate of falloff of the angular distribution are determined, respectively, by the “black-disk” size of the nucleus  $\bar{b}$  and the slope of the density in the nuclear surface, respectively. For pions,  $\bar{b}$  corresponds to the distance from the center of the nucleus at which the density has fallen to about 10% of its central value [2], which is in turn determined by both the radius and diffuseness of the density. Thus, the diffractive pattern of the elastic scattering angular distribution provides a means to assess gross properties of the density distribution, as demonstrated in Ref. [23]. The sensitivity of the elastic scattering to changes in the radius is shown in Fig. 8(a), which confirms the general trends expected. Changing the radius has a similar effect on the diffraction pattern for excitation of the  $2^+$  state, as shown in Fig. 8(b).

Additionally, the scattering to the  $2^+$  state is quite sensitive to the neutron and proton deformation parameters. The main purpose of this section is to provide a quantitative measure of the relative sensitivity of the  $2^+$  angular distribution to the radius and deformation properties of the density.

Sensitivity to changes in  $\beta_2$  is shown in Fig. 9 for scattering to the first  $2^+$  state. We find that the deformation parameters have negligible effect on the elastic scattering angular distribution, consistent with the findings in Sec. IV that the elastic scattering is insensitive to the coupling of the excited rotational levels. The results we find here are similar to the sensitivity studies made in Ref. [24] using the Eikonal approximation with the density expansion given in our Eq. (3.2).

We see from Figs. 8(b) and 9 that the overall magnitude of the inelastic scattering of  $\pi^-$  to the  $2^+$  state will be determined predominantly by the neutron deformation. Excitation of the  $2^+$  by the  $\pi^+$  will be similarly de-

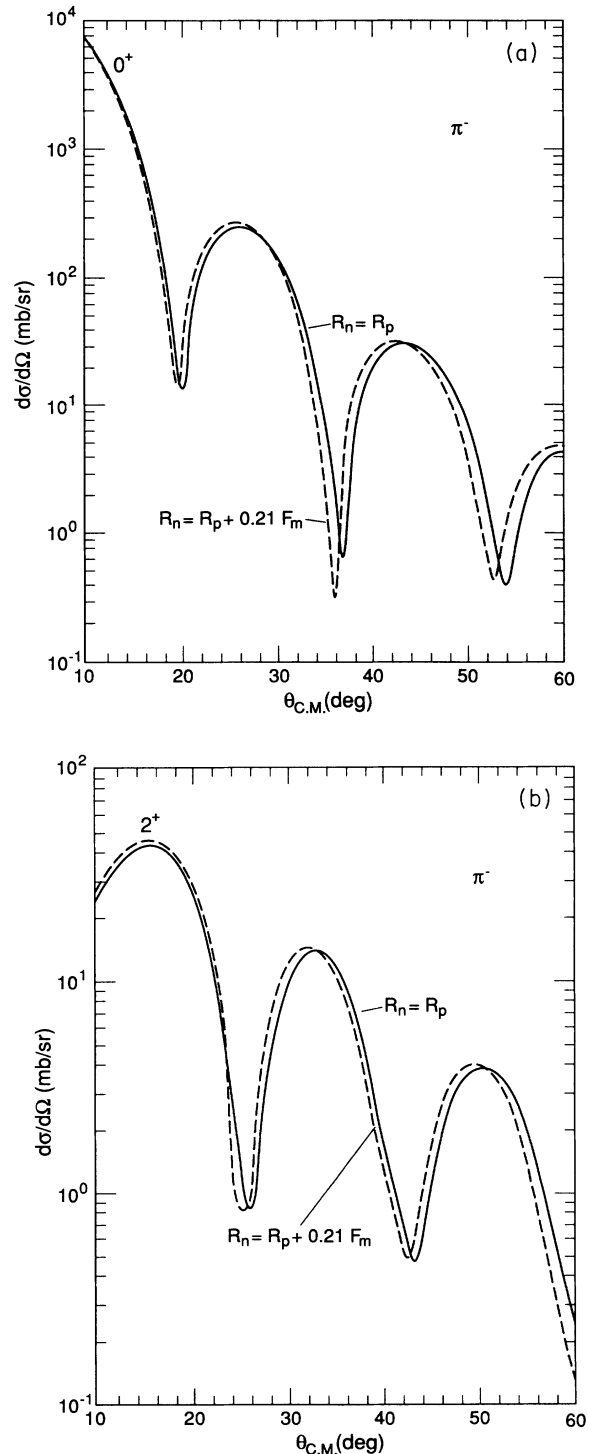


FIG. 8. Sensitivity of the  $\pi^-$  (a) elastic and (b)  $2^+$  cross section to changes in the neutron radius constant  $R_{0n}$  of the parametrized Woods-Saxon density used.



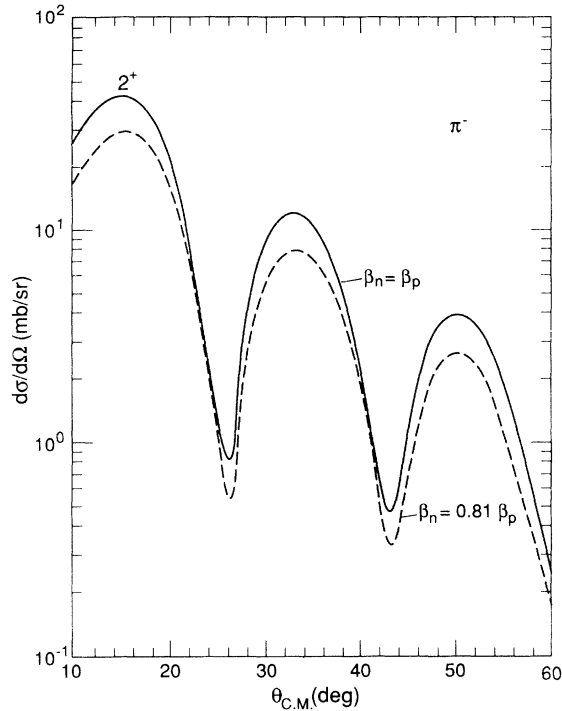


FIG. 9. Sensitivity of the  $\pi^- 2^+$  cross section to changes in the quadrupole deformation parameter  $\beta_{2n}$  of the parameterized Woods-Saxon density used.

terminated largely by the proton deformation. This sensitivity can be understood in terms of the discussion at the end of Sec. II, where it was observed that the strength of the transition potential to the  $2^+$  state is proportional to the  $\lambda = 2$  multipole component of the optical potential, to the extent that channel-coupling effects and medium modifications can be ignored. (We showed in Secs. III and V that the reorientation coupling and medium modifications each constitute about a 10% correction to this picture.) On the other hand, scattering to the  $4^+$  state would not cleanly reflect the  $\beta_4$  parameter because of the strong interference between the different amplitudes previously noted in Sec. IV and because of the sensitivity to medium modifications displayed in this channel, noted in Sec. V.

We have not separately studied the sensitivity to the diffuseness, but we know from previous studies of diffractive scattering [23] that changing the diffuseness will affect both the apparent radius of the nucleus (increasing the diffuseness moves out the 10% density point, making the nucleus look larger) and at the same time smooth out the shape of the density, so that the cross section falls off more rapidly with momentum transfer [25].

The results of this section are in qualitative agreement with the earlier results of Ref. [3]. At the quantitative level there are differences. Two significant improvements in the present work are the inclusion of medium modifications and reorientation coupling. Additionally, as we have remarked already, excited states play a less significant role in our theory than they did in Ref. [3].

## VII. SUMMARY AND CONCLUSIONS

We undertook the current investigation to establish the applicability of our microscopic coupled-channel theory of pion inelastic scattering for the purpose of distinguishing details of neutron and proton densities. The theoretical framework is based upon a microscopic optical model for the form originally suggested by Ericson and Ericson [11]. The optical potential for elastic and charge exchange [14] is expressed as a functional of the neutron, proton, and transition densities with the isoscalar and isovector potentials consisting of terms linear and quadratic in the appropriate nuclear densities. The strengths of the various terms were determined from theoretical arguments and from phenomenological studies of elastic and charge-exchange data. The same optical-potential parameters are to be used in applying the theory to rotational nuclei as described in this paper.

The nuclear densities that we use in the current paper are taken from the Hartree-Fock theory of deformed nuclei using the SKM\* interaction [8]. This theory completely determines the ground-state and transition densities that are needed in order to calculate elastic and inelastic cross sections. Thus, with this additional information we have a complete theory with which to make our study of inelastic scattering.

To solve the three-dimensional Klein-Gordon equation for pion scattering on deformed nuclei, we first make a multipole expansion of the HF densities and pion wave functions. We obtain an equivalent set of coupled one-dimensional radial equations expressed in terms of these quantities, which we solve to obtain the scattering from the ground state and to the excited rotational levels of  $^{152}\text{Sm}$ .

In our study of the convergence of the theory, we found: (1) convergence in terms of multipole components of the HF densities is favorable. Results for the elastic scattering change by less than a percent and cross sections to the  $2^+$  decrease by about 30% at the maxima when higher multipoles are added. (2) Convergence of the cross sections for elastic and inelastic scattering to the first  $2^+$  state with respect to the number of intermediate rotational coupled nuclear levels is also rapid and more favorable than that found in previous work [3]. Contrary to what is found for pion single charge exchange [5], the medium modifications have a moderately small effect, raising the inelastic cross sections by about 10% for  $\pi^-$  and  $\pi^+$  for the scattering to the  $2^+$  state. We also studied inelastic scattering to the  $4^+$  state, which we found to be quite sensitive to both medium modifications and to coupling through the  $2^+$  channel; we conclude that the experimental study of the  $4^+$  state would be quite interesting for these reasons. Our study also confirms the expected sensitivity of pion scattering cross sections to variations in the size and shape of the neutron and proton distribution.

Our overall conclusion is that the microscopic coupled-channel theory is well behaved for applications to inelastic scattering. For the purpose of applying the theory to assess models of nuclear densities one must be aware that the differences between models are relatively small,

so that 10% effects must be considered significant. Since we have found that for scattering to the  $2^+$  state medium modifications are of this size, and the reorientation coupling is substantially larger, a theory such as the one we use must be employed in such applications. However, since they affect  $\pi^+$  and  $\pi^-$  in the same way, they are much more important for assessing isoscalar properties than isovector properties, such as neutron/proton deformations differences. We have made use of the results presented in this work for such a study of Hartree-Fock densities using the experimental data [3] in Ref. [10].

## ACKNOWLEDGMENTS

This work was partially supported by the U.S. Department of Energy. We gratefully acknowledge the hospitality extended by the University of Munich (to J.B.) and by the Institute for Nuclear Theory at the University of Washington (to M.B.J. and W.S.), where parts of the work were completed. We also express our appreciation to G. R. Satchler for his helpful critique of the manuscript.

- 
- [1] M. K. Jakobson *et al.*, Phys. Rev. Lett. **38**, 1201 (1977)
- [2] M. B. Johnson and H. A. Bethe, Comm. Nucl. Part. Phys. **8**, 75 (1978).
- [3] C. L. Morris *et al.*, Phys. Rev. C **28**, 2165 (1983).
- [4] J. N. Knudson *et al.*, Phys. Rev. Lett. **66**, 1026 (1991).
- [5] J. Bartel, M. B. Johnson, and M. K. Singham, Ann. Phys. (N.Y.) **196**, 89 (1989).
- [6] R. D. Amado, Adv. Nucl. Phys. **10**, 1 (1985).
- [7] Y. Abgrall, R. Belaidi, and J. Labarsouque, Nucl. Phys. **A426**, 781 (1987).
- [8] J. Bartel, P. Quentin, M. Brack, C. Guet, and H. B. Hakansson, Nucl. Phys. **A386**, 79 (1982).
- [9] P. Quentin and H. Flocard, Annu. Rev. Nucl. Part. Sci. **28**, 523 (1978).
- [10] J. Bartel, M. B. Johnson, M. K. Singham, and W. Stocker, Phys. Lett. B **296**, 5 (1992).
- [11] T. E. O. Ericson and M. Ericson, Ann. Phys. (N.Y.) **36**, 323 (1966).
- [12] E. R. Siciliano, M. D. Cooper, M. B. Johnson, and M. J. Leitch, Phys. Rev. C **34**, 267 (1986).
- [13] S. J. Green *et al.*, Phys. Rev. C **30**, 2003 (1984).
- [14] M. B. Johnson and E. R. Siciliano, Phys. Rev. C **27**, 730 (1983); **27**, 1647 (1983).
- [15] For  $\lambda > 0$ , the approximation of linearizing the transition optical potential breaks down for large deformations [16]. For  $^{152}\text{Sm}$  we estimate that it underestimates effects of medium modifications by about 30% for  $2^+$  states. It does not change the conclusions of our work because the medium modifications (see Sec. V) are only about 10% for the  $2^+$  transitions shown there.
- [16] We thank G. R. Satchler for a discussion on this point.
- [17] The slightly different values of the  $\beta_2$  given in Ref. [10] were obtained for sharp surface distribution [see Ref. [5], Eq. (3.2.6) and associated discussions] whereas in the present work the  $\beta_\lambda$  were determined from the diffuse-surface Woods-Saxon distributions.
- [18] See also G. R. Satchler, *Direct Nuclear Reactions* (Oxford University Press, New York, 1983), Chap. 14.2.
- [19] N. Austern, R. M. Drisco, E. Rost, and G. R. Satchler, Phys. Rev. **128**, 733 (1962).
- [20] G. R. Satchler, J. L. Yntema, and H. W. Broek, Phys. Lett. B **12**, 55 (1964).
- [21] We thank C. Morris for a clarifying discussion of this point.
- [22] M. B. Johnson and D. J. Ernst, Ann. Phys. (N.Y.) **219**, 266 (1992).
- [23] J.-F. Germond, M. B. Johnson, and J. Johnstone, Phys. Rev. C **32**, 983 (1985).
- [24] Z. Yushun, Chin. J. Nucl. Phys. **14**, 201 (1992).
- [25] E. V. Inopin and Yu. A. Berezhnoy, Nucl. Phys. **63**, 689 (1965).